

Effects of Longitudinal Fluctuations in Heavy-Ion Collisions

Rashmi Raniwala, Sudhir Raniwala

Physics Department, University of Rajasthan, Jaipur, India

Constantin Loizides

Lawrence Berkeley National Laboratory, Berkeley, California, USA

Abstract

In collisions of identical nuclei at a given impact parameter, the number of nucleons participating in the overlap region of each nucleus can be unequal due to nuclear density fluctuations. The asymmetry due to the unequal number of participating nucleons, which may be experimentally accessible by measuring either the energy in ZDC or the number of spectator nucleons, causes a shift of the center of mass rapidity of the participant zone. In a Monte Carlo Glauber model the average rapidity-shift is found to be almost linearly related to the asymmetry. Using Monte Carlo data for Pb–Pb collisions at 2.76 TeV generated with the HIJING model, we demonstrate that the rapidity distribution of produced particles is affected by the asymmetry, and that the effect can be quantitatively related to the average rapidity-shift via a third-order polynomial with a dominantly linear term. Experimental estimates of the spectator asymmetry may be used to further constrain the initial conditions in ultra-relativistic heavy ion collisions.

1. Introduction

In collisions of heavy ions the geometrically overlapping region created by interacting nucleons from each nucleus is called the participant zone. Even at fixed impact parameter, the number of participating nucleons from each nucleus fluctuates around the mean due to fluctuations in the positions of the nucleons around the mean nuclear density profile. Event-by-event, the participant zone therefore has a net non-zero momentum in the nucleon-nucleon centre-of-mass (CM) frame, and hence its rapidity is shifted with respect to the CM frame [1].

Experimental data and simulated data from different event generators show that the total produced particle multiplicity, measured in a wide phase-space region, scales approximately with the number of participants [2, 3]. The observed N_{part} scaling indicates that the number of participants is a relevant parameter affecting the production and distribution of produced particles even at LHC energies. Recently, fluctuations in the number of participants from each nucleus have been shown to be correlated with forward-backward multiplicity fluctuations [4]. The distribution of charged particles averaged over a large

number of events in collisions of identical nuclei is observed to be symmetric about the rapidity of the nucleon-nucleon CM frame. In the present work, we investigate the possible effect of the net (non-zero) momentum of the participant zone on experimentally measurable distributions of produced particles by exploring possible correlations between the participant asymmetry and the distribution of particles in the kinematic phase space. Preliminary results of the ALICE collaboration show a difference between pseudorapidity distribution of charged particles in events of different asymmetries, as estimated from the measurement of spectator neutrons [5]. The similar transverse-momentum dependence of the rapidity-even directed flow and the corresponding estimate from two-particle correlations at mid-rapidity indicate a weak correlation between fluctuating participant and spectator symmetry planes and suggest the possibility of using the spectator nucleons to further determine and constrain the effect of initial conditions [6].

The paper is organised as follows. The rapidity-shift of the participant zone due to asymmetry of the event is discussed in Section 2. For a Gaussian charged particle rapidity distribution, the effect of constant rapidity-shift is estimated using a toy model and is discussed in Section 3. Section 4 discusses the effect on various charged particle rapidity distributions for variable rapidity-shifts. The results of the present work are summarised in Section 5.

2. Rapidity Shift of Participant Zone

If the number of nucleons participating from the two colliding nuclei is A and B , respectively, then the participant zone has a net momentum in the nucleon-nucleon CM frame. The net momentum corresponds to a shift in the rapidity of the participant zone, which can be approximated as

$$y_0 \cong \frac{1}{2} \ln \frac{A}{B}. \quad (1)$$

Assuming each of the A (B) nucleons has a fixed momentum p ($-p$), Eq. 1 is obtained using the sum of four-momentum vectors $(0, 0, Ap, AE)$ and $(0, 0, -Bp, BE)$, with $E^2 = m_0^2 + p^2$, and neglecting $m_0 \ll p$. Since at the LHC in the TeV scale, $m_0/p < 10^{-6}$, we replace the ' \cong ' sign by the equality sign hitherto.

Defining the asymmetry of participants for each event as $\alpha_{\text{part}} = \frac{A-B}{A+B}$, the rapidity-shift y_0 can be written as

$$y_0 = \frac{1}{2} \ln \frac{1 + \alpha_{\text{part}}}{1 - \alpha_{\text{part}}}, \quad (2)$$

and is uniquely determined for a given α_{part} . For small α_{part} , the shift follows $y_0 \cong \alpha_{\text{part}}$. The unequal number of nucleons in the participant zone imply unequal number of spectators of the two colliding nuclei, $N - A$ and $N - B$, respectively, where N is the total number of nucleons in each nucleus. The spectator asymmetry $\alpha_{\text{spec}} = \frac{(N-A)-(N-B)}{(N-A)+(N-B)} = \frac{B-A}{2N-(A+B)}$ is related to the participant asymmetry via $\alpha_{\text{spec}} = -\alpha_{\text{part}} \frac{A+B}{2N-(A+B)}$. Finally, the rapidity shift y_0 is related to the spectator asymmetry as

$$y_0 = \frac{1}{2} \ln \frac{(A+B)(1 + \alpha_{\text{spec}}) - 2N\alpha_{\text{spec}}}{(A+B)(1 - \alpha_{\text{spec}}) + 2N\alpha_{\text{spec}}}. \quad (3)$$

2

Centrality	b_{\min} (fm)	b_{\max} (fm)	$\langle N_{\text{part}} \rangle$	$\langle y_0 \rangle$
0–5%	0.0	3.61	383.9	0.0144
5–10%	3.61	5.12	330.0	0.0263
10–15%	5.12	6.27	280.2	0.0352
15–20%	6.27	7.24	236.5	0.0431
20–25%	7.24	8.09	198.5	0.0512
25–30%	8.09	8.86	165.5	0.0589
30–35%	8.86	9.57	136.5	0.0678
35–40%	9.57	10.23	110.2	0.0777
40–45%	10.23	10.85	88.6	0.0887
45–50%	10.85	11.43	70.2	0.1012
50–55%	11.43	11.99	54.6	0.1155
55–60%	11.99	12.52	41.6	0.1326
60–65%	12.52	13.03	31.0	0.1528
65–70%	13.03	13.52	22.5	0.1764

Table 1: Centrality classes defined by impact parameter as well as corresponding $\langle N_{\text{part}} \rangle$ and $\langle |y_0| \rangle$ values.

Unlike the unique correspondence between α_{part} and y_0 , the presence of the $(A + B)$ term in Eq. 3 leads to a distribution of y_0 for a given value of α_{spec} , even at fixed impact parameter or centrality.

The rapidity-shift y_0 (Eq. 1) as well as its dependence on α_{part} (Eq. 2) and α_{spec} (Eq. 3) can be calculated within a Monte Carlo Glauber (MCG) framework [7], as implemented in Refs. [8, 9] or in Ref. [10]. In the present work, we have generated 1.4 million minimum bias events of Pb–Pb collisions at $\sqrt{s_{\text{NN}}} = 2.76$ TeV using HIJING (v1.383) [10] with default settings. The generated impact parameter (b) is used to define the event centrality. Limits on b used for 5%-wide centrality intervals with corresponding $\langle N_{\text{part}} \rangle$ are provided in Tab. 1. The mean number of participants provide an estimate of the order of magnitude of the rapidity-shift. Assuming that the number of nucleons from each of the two nuclei fluctuate by their root mean square while retaining the total number to be equal to N_{part} , the resulting value of rapidity shift for the most central class of events would be as large as ≈ 0.05 . In practice, events in any centrality class will have a distribution peaked at zero. The distributions of y_0 , α_{part} and α_{spec} calculated with the HIJING MCG are shown in Fig. 1 for three centrality classes along with a Gaussian fit for each. The width of the y_0 distribution increases with decreasing centrality, i.e. for larger impact parameters the relative fluctuations increase since the number of participants decreases. Events can be classified according to their rapidity-shift: $y_0 < 0$ are events of negative asymmetry (*-asym*) and $y_0 > 0$ are events of positive asymmetry (*+asym*). For each centrality class, the mean value of $|y_0|$ is also reported in Tab. 1. The increase of $|y_0|$ with decreasing collision centrality is in agreement with results obtained earlier [1]. The α_{part} distributions are nearly identical to the y_0 distributions,

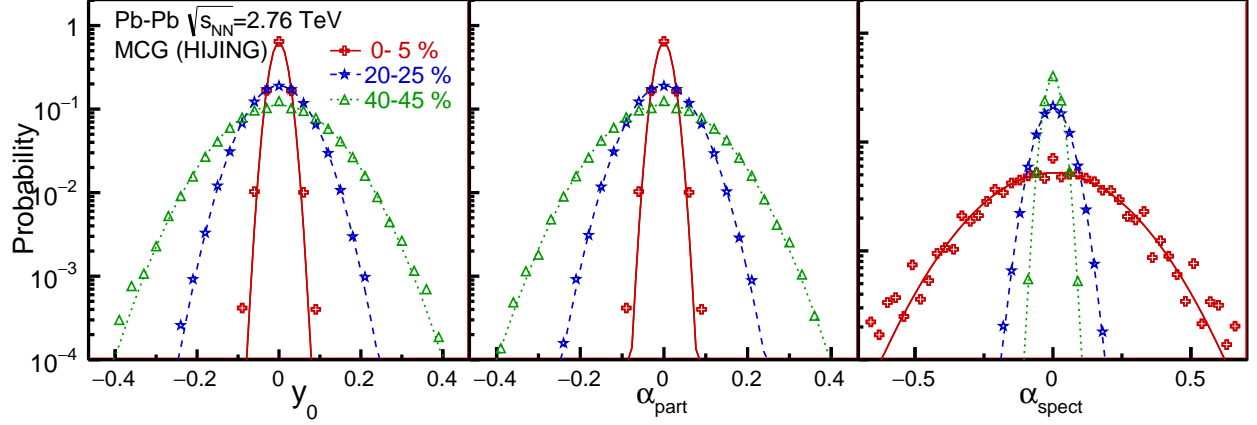


Figure 1: The distributions of the participant-zone rapidity shift y_0 (left panel), of the participant asymmetry α_{part} (middle panel) and of the spectator asymmetry α_{spec} for 0–5%, 20–25% and 40–45% Pb–Pb centrality classes calculated with the HIJING MCG.

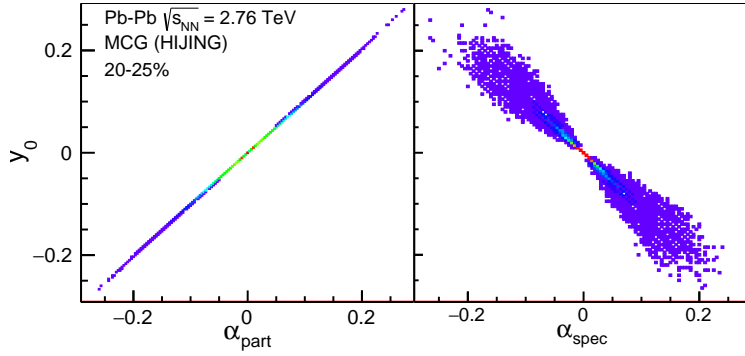


Figure 2: Event-by-event distributions of y_0 versus α_{part} (left panel) and y_0 versus α_{spec} for the 20–25% Pb–Pb centrality class calculated with the HIJING MCG.

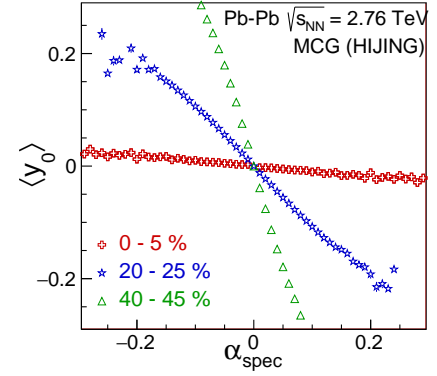


Figure 3: $\langle y_0 \rangle$ versus α_{spec} for 0–5%, 20–25% and 40–45% Pb–Pb .

while the α_{spec} distributions are different. The widths of the α_{spec} distributions increase with increasing centrality, i.e. the relative fluctuations increase with decreasing number of spectating nucleons.

Figure 2 displays event-by-event distributions of y_0 versus α_{part} and α_{spec} , respectively, obtained for the 20–25% Pb–Pb centrality class with the HIJING MCG. The unique correspondence between y_0 and α_{part} is illustrated in the left panel of Fig. 2. The lack of a unique relation between y_0 and α_{spec} due to the presence of the $(A + B)$ term in Eq. 3 leads to a distribution of y_0 for a given value of α_{spec} , even at fixed impact parameter or centrality, as illustrated in the right panel of Fig. 2. It can be regarded as the response matrix to obtain the values of $\langle y_0 \rangle$ for a given range of α_{spec} . The mean values $\langle y_0 \rangle$ as a function of the α_{spec} asymmetry are shown in Fig. 3 for three different centralities for 0–5%, 20–25% and 40–45%

Pb–Pb centrality classes calculated with the HIJING MCG.

If the experiments could measure the number of nucleons in the participant zone, A and B , the participant-zone rapidity shift y_0 could be determined for each collision. However, neither A and B , nor α_{part} is directly amenable to experimental measurement. The asymmetry α_{spec} can be estimated by measuring the number of spectator nucleons through their energy deposited in the zero degree calorimeters on either side of the interaction vertex in collider experiments. Via unfolding methods one may be able to obtain an estimate of $\langle y_0 \rangle$, e.g. by using the response matrix in the right panel of Fig. 2.

3. Constant Rapidity Shift and Gaussian Charged Particle Rapidity Distribution

The measured rapidity distribution of charged particles produced in collisions of identical nuclei can be described by distributions, which are symmetric about the CM rapidity [2, 3]. A Gaussian form is amongst the more common distributions used to describe data. We assume that the particles produced in asymmetric collisions of identical nuclei are also distributed symmetrically in the CM frame of the participant zone. Considering that the rapidity of the participant zone is shifted by y_0 from the rapidity of the nucleon-nucleon CM system, a symmetric distribution in the participant zone will appear as a shifted distribution in the nucleon-nucleon CM frame, which is also the laboratory frame for most collider experiments. For fixed y_0 , the rapidity distributions of produced particles can be written as

$$\frac{dN}{dy} = N_0 \exp\left(-\frac{(y - y_0)^2}{2\sigma^2}\right). \quad (4)$$

For symmetric collisions $y_0 = 0$, while for longitudinally asymmetric collisions y_0 is finite. The positive and negative values of y_0 correspond to the net momentum of the participant zone in the positive and negative direction, respectively, causing positive and negative participant (α_{part}) asymmetries, respectively. The ratio of the rapidity distribution of particles in collisions with positive asymmetry to the distribution in collisions of negative asymmetry yields

$$\begin{aligned} \frac{\left(\frac{dN}{dy}\right)_{+\text{asym}}}{\left(\frac{dN}{dy}\right)_{-\text{asym}}} &= \exp\left(\frac{4yy_0}{\sigma^2}\right) \\ &= \sum_{n=0}^{\infty} c_n^g(y_0, \sigma) y^n, \end{aligned} \quad (5)$$

where $c_n^g = (4y_0/\sigma^2)^n/n!$ are the coefficients of the Taylor expansion of the exponential function, and the superscript g of the coefficients stands for the Gaussian shape of the parent rapidity distribution. The coefficients depend upon the parameters of the parent rapidity distribution and on the rapidity shift y_0 . For typical values of y_0 equal to 0.1 and σ equal to 3.6, the ratio $\frac{c_2^g}{c_1^g} \sim 0.015$ and the ratio $\frac{c_3^g}{c_1^g} \sim 0.00015$ with subsequent terms having negligible contribution to the values of the function describing the ratio of the two rapidity

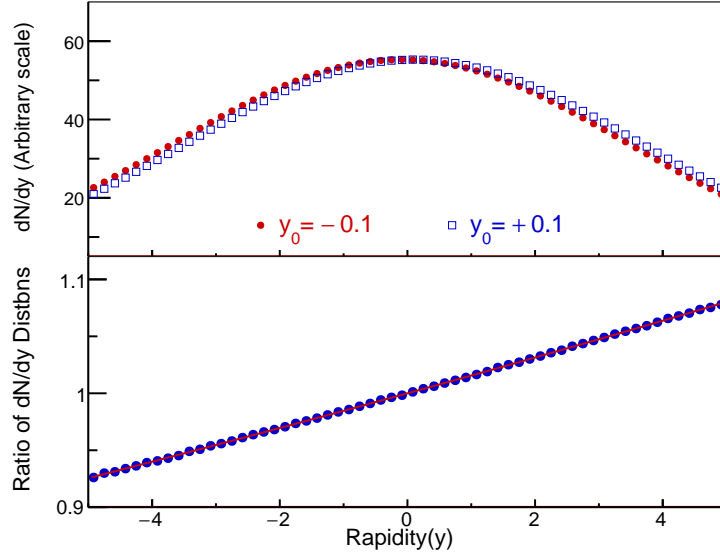


Figure 4: Gaussian $\frac{dN}{dy}$ distributions for $\sigma = 3.6$ shifted by $y_0 \pm 0.1$ obtained by the toy model (top panel). Ratio of the $\frac{dN}{dy}$ distributions fitted to a third-order polynomial (bottom panel). The coefficients are 0.015, 1.1×10^{-4} and 2.2×10^{-7} , respectively with $\chi^2/\text{dof} = 125/117$.

distributions. Hence, for a Gaussian rapidity distribution, where the relation between the shift of the participant-zone rapidity and the coefficients c_n are analytically known, the dominant contribution can be expected for the linear term. The linear term is related to the rapidity-shift via $y_0 = \frac{c_1^9 \sigma^2}{4}$.

These results have been validated using a toy model simulation by generating Gaussian rapidity distributions which are shifted by a constant magnitude. The top panel of Fig. 4 shows two rapidity distributions for $\sigma = 3.6$ shifted by $y_0 \pm 0.1$. The unshifted distribution would obviously lie in between the two distributions and is not drawn. The bottom panel of Fig. 4 shows the ratio of $\frac{dN}{dy}$ distributions for events with $y_0 = +0.1$ to those with $y_0 = -0.1$, and the ratio is fitted to a third-order polynomial. The coefficient of the linear term is dominant with the other coefficients smaller by 2 and 4 orders of magnitude, respectively, as expected from Eq. 5. The same calculation is repeated for different values of the shift y_0 to obtain the coefficients of the third-order polynomial fit as function of y_0 , as shown in Fig. 5. The dependence of the coefficients on the rapidity-shift known from Eq. 5 is indicated with dashed lines, and agrees very well with the numerical calculation. The figure demonstrates that the dominant contribution to the $\frac{dN}{dy}$ ratio arises from the first coefficient, which is linearly related to the rapidity shift y_0 .

4. Variable Shift and Various Charged Particle Rapidity Distributions

In the previous section we discussed the relation of coefficients of the third-order polynomial fit to the ratio of $\frac{dN}{dy}$ distributions assuming that the $\frac{dN}{dy}$ distributions are Gaussian

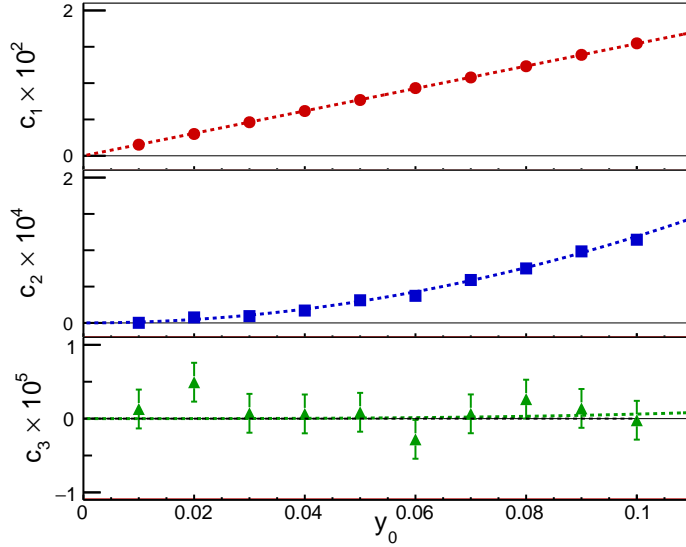


Figure 5: The dependences of c_1^g , c_2^g and c_3^g on y_0 for fixed $\sigma = 3.6$ obtained by the toy model. Dashed lines correspond to analytical functions of the coefficients from Eq. 5.

in nature, and that all events have the same positive or negative y_0 . In the following, the values of y_0 for different events are chosen according to the distribution of y_0 from the HIJING MCG, as shown for a few centrality classes in the left panel of Fig. 1. As before, the rapidity distribution of particles $\frac{dN}{dy}$ are generated using a toy simulation taking into account event-by-event the rapidity-shift y_0 .

In addition to a Gaussian distribution, we also consider that the rapidity of produced particles can be described by a Woods-Saxon distribution

$$\frac{dN}{dy} = N_0 \frac{1}{1 + \exp\left(\frac{|(y-y_0)|-a}{c}\right)} \quad (6)$$

where $y_0 = 0$ for symmetric events, positive for events with positive asymmetry, and negative for events with negative asymmetry. Taking the ratio of the $\frac{dN}{dy}$ for events of opposite asymmetry, and making a Taylor expansion about $y = 0$ yields a polynomial in y , which can be written as

$$\frac{\left(\frac{dN}{dy}\right)_{+\text{asym}}}{\left(\frac{dN}{dy}\right)_{-\text{asym}}} = \sum_{n=0}^{\infty} c_n^{\text{ws}}(y_0, a, c) y^n. \quad (7)$$

The coefficients c_n^{ws} depend on the shift in rapidity and the parameters of the Woods-Saxon distribution in a non-trivial way. For a given set of parameters, however, the dependence on the rapidity-shift y_0 could be computed numerically.

We investigate the systematic effect of the coefficients on rapidity-shift for different commonly used rapidity distributions: Gaussian, Woods-Saxon and the charged-particle rapidity

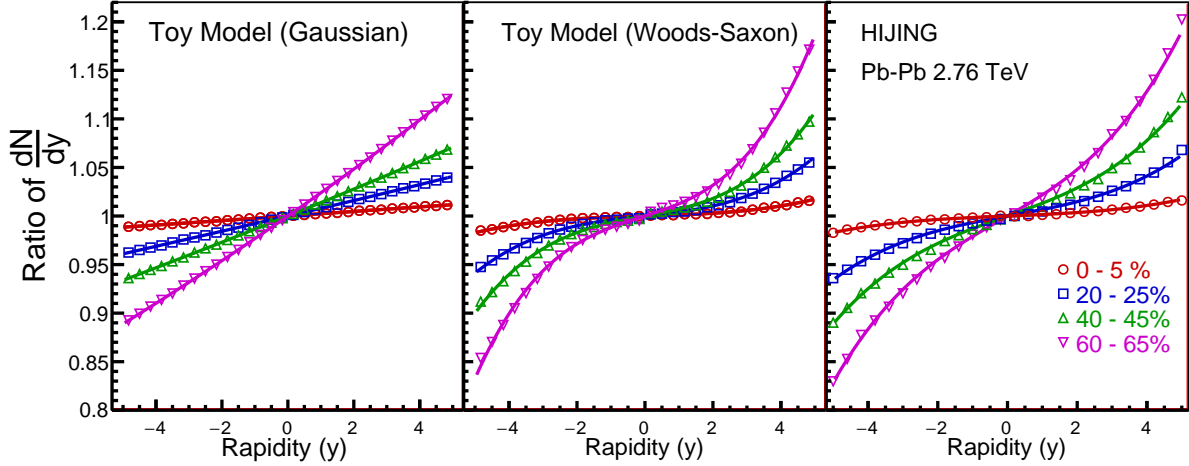


Figure 6: The ratio of $\frac{dN}{dy}$ distributions for events with positive ($y_0 > 0$) and with negative ($y_0 < 0$) asymmetry for Gaussian (left panel), Wood-Saxon (middle panel) and HIJING (right panel) rapidity distributions for four centrality classes. The ratios are fitted to third-order polynomials.

distribution resulting from HIJING. Using the parameterized form of experimental η and p_T distributions in conjunction with the relative yield of pions, kaons and protons [3, 11], simulations provided the rapidity distribution. The resulting $\frac{dN}{dy}$ distribution is fitted to a Gaussian form and to a Woods-Saxon form to obtain the value of the parameters. The HIJING events are for Pb-Pb collisions at $\sqrt{s_{NN}} = 2.76$ TeV with default settings. The rapidity distributions are obtained separately for positive and negative values of y_0 in various centrality classes, and their ratios are fitted to third-order polynomials, as shown in Fig. 6 for four centrality classes. In each of the three cases, the χ^2/dof are the smallest in the most central class and are about 0.64, 0.83 and 0.74 for Gaussian, Wood-Saxon and HIJING, respectively.

The dependence of the first three coefficients c_n on the mean rapidity shift $\langle |y_0| \rangle$ is shown in Fig. 7. We find the linear term for HIJING to be closer to the correspond term of the Gaussian than for the Woods-Saxon rapidity distribution. For all distributions, the coefficients for the quadratic and cubic terms are much smaller than those of the linear term. While the coefficient of the cubic term for the Gaussian rapidity distribution is zero, those of the Woods-Saxon distribution and of HIJING show quantitatively similar behaviour, with a nearly linear dependence on $\langle |y_0| \rangle$.

5. Summary

In collisions of identical nuclei at a given impact parameter, the number of nucleons participating in the overlap region of each nucleus estimated with a Monte Carlo Glauber can be unequal due to nuclear density fluctuations (Fig. 1). The asymmetry due to the unequal

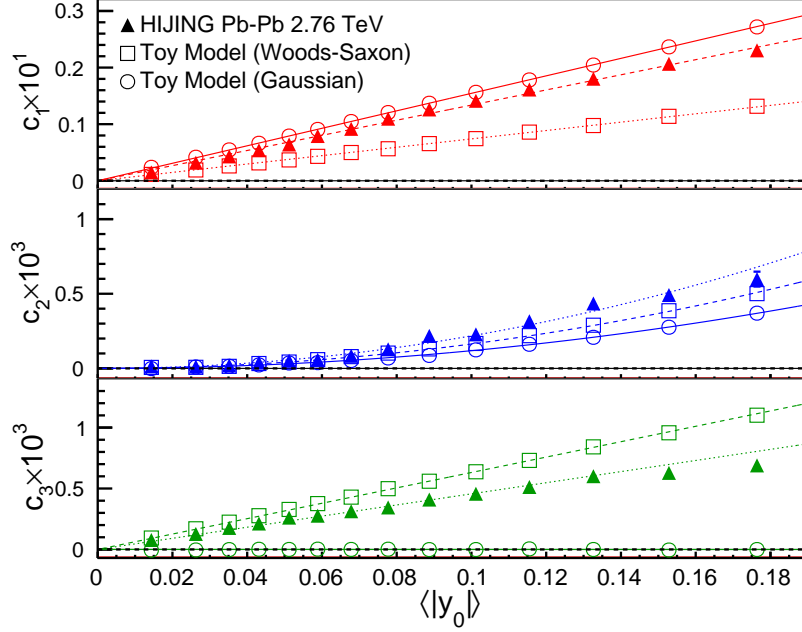


Figure 7: The coefficients c_1 , c_2 , and c_3 of the third-order polynomial fit to the ratio of $\frac{dN}{dy}$ distributions versus $\langle |y_0| \rangle$ for the Gaussian, Wood-Saxon and HIJING rapidity distributions. The rapidity distributions are obtained in 14 centrality intervals up to 70% centrality with corresponding $\langle |y_0| \rangle$ as given in Tab. 1. Linear fits are shown for c_1 and c_3 , and a quadratic fit for c_2 . These fits are only to guide the eye.

number of participating nucleons causes a rapidity-shift of the participant zone (Fig. 2), which may be experimentally accessible by measuring the energy of the spectator nucleons. The average rapidity-shift has been found to be almost linearly related to the asymmetry (Fig. 3). A toy model, in which the rapidity distribution of charged particles is described by a Gaussian distribution, has been used to illustrate that the ratio of rapidity distributions for positive and negative asymmetry can effectively be described by a third-order polynomial (Fig. 4). The dependence of the coefficients for a fixed rapidity-shift has been extracted (Fig. 5). The effect on the ratio of rapidity distributions for positive and negative asymmetry has been systematically studied using Monte Carlo data for Pb-Pb collisions at 2.76 TeV generated with the HIJING model for a variety of centrality classes, as well as with the toy model for Gaussian and Wood-Saxon particle rapidity distributions and the rapidity-shift distribution taken from HIJING. The ratios turn out to be sensitive to the detailed shape of the parent rapidity distribution (Fig. 6), and can be quantitatively described by a third-order polynomial with a dominantly linear term (Fig. 7). Experimentally, estimates of the longitudinal asymmetry via measurements of the spectator asymmetry can be used to systematically investigate the influence of the longitudinal asymmetry on various observables, and hence may further constrain the initial conditions in ultra-relativistic heavy ion collisions.

6. Acknowledgements

We thank Jurgen Schukraft for fruitful discussions. R. Raniwala and S. Raniwala acknowledge the financial support of the Department of Science and Technology of the Government of India. The work of C. Loizides is supported in part by the U.S. Department of Energy, Office of Science, Office of Nuclear Physics, under contract number DE-AC02-05CH11231.

References

References

- [1] V. Vovchenko, D. Anchishkin, L. P. Csernai, Longitudinal fluctuations of the center of mass of the participants in heavy-ion collisions, Phys. Rev. C88 (1) (2013) 014901. [arXiv:1306.5208](#), doi:10.1103/PhysRevC.88.014901.
- [2] B. Alver, et al., Phobos results on charged particle multiplicity and pseudorapidity distributions in Au–Au, Cu–Cu, d–Au, and pp collisions at ultra-relativistic energies, Phys. Rev. C83 (2011) 024913. [arXiv:1011.1940](#), doi:10.1103/PhysRevC.83.024913.
- [3] E. Abbas, et al., Centrality dependence of the pseudorapidity density distribution for charged particles in Pb–Pb collisions at $\sqrt{s_{NN}} = 2.76$ TeV, Phys. Lett. B726 (2013) 610–622. [arXiv:1304.0347](#), doi:10.1016/j.physletb.2013.09.022.
- [4] J. Jia, S. Radhakrishnan, M. Zhou, Forward-backward multiplicity fluctuation and longitudinal harmonics in high-energy nuclear collisions, Phys. Rev. C93 (4) (2016) 044905. [arXiv:1506.03496](#), doi:10.1103/PhysRevC.93.044905.
- [5] R. Raniwala, Longitudinal asymmetry and its measurable effects in Pb–Pb collisions at 2.76 TeV, in: 25th International Conference on Ultra-Relativistic Nucleus-Nucleus Collisions (Quark Matter 2015) Kobe, Japan, September 27–October 3, 2015, 2015. [arXiv:1512.08177](#). URL <http://inspirehep.net/record/1411530/files/arXiv:1512.08177.pdf>
- [6] B. Abelev, et al., Directed flow of charged particles at midrapidity relative to the spectator plane in Pb–Pb collisions at $\sqrt{s_{NN}}=2.76$ TeV, Phys. Rev. Lett. 111 (23) (2013) 232302. [arXiv:1306.4145](#), doi:10.1103/PhysRevLett.111.232302.
- [7] M. L. Miller, K. Reygers, S. J. Sanders, P. Steinberg, Glauber modeling in high energy nuclear collisions, Ann. Rev. Nucl. Part. Sci. 57 (2007) 205–243. [arXiv:nuc1-ex/0701025](#), doi:10.1146/annurev.nucl.57.090506.123020.
- [8] B. Alver, M. Baker, C. Loizides, P. Steinberg, The PHOBOS Glauber Monte Carlo [arXiv:0805.4411](#).
- [9] C. Loizides, J. Nagle, P. Steinberg, Improved version of the PHOBOS Glauber Monte Carlo, SoftwareX 1-2 (2015) 13–18. [arXiv:1408.2549](#), doi:10.1016/j.softx.2015.05.001.
- [10] X.-N. Wang, M. Gyulassy, HIJING: A Monte Carlo model for multiple jet production in pp, pA and AA collisions, Phys. Rev. D44 (1991) 3501–3516. doi:10.1103/PhysRevD.44.3501.
- [11] B. Abelev, et al., Centrality dependence of π , K, p production in Pb–Pb collisions at $\sqrt{s_{NN}} = 2.76$ TeV, Phys. Rev. C88 (2013) 044910. [arXiv:1303.0737](#), doi:10.1103/PhysRevC.88.044910.